89Zr-bevacizumab PET visualizes heterogeneous tracer accumulation in tumor lesions of renal cell carcinoma patients and differential effects of antiangiogenic treatment

Oosting, Sjoukje F; Brouwers, Adrienne H; van Es, Suzanne C; Nagengast, Wouter B; Oude Munnink, Thijs H; Lub-de Hooge, Marjolijn N; Hollema, Harry; de Jong, Johan R; de Jong, Igle J; de Haas, Sanne

Published in:
Journal of Nuclear Medicine

DOI:
10.2967/jnumed.114.144840

Document Version
Publisher's PDF, also known as Version of record

Publication date:
2015

^{89}Zr-Bevacizumab PET Visualizes Heterogeneous Tracer Accumulation in Tumor Lesions of Renal Cell Carcinoma Patients and Differential Effects of Antiangiogenic Treatment

Sjoukje F. Oosting[1], Adrienne H. Brouwers[2], Suzanne C. van Es[1], Wouter B. Nagengast[3], Thijs H. Oude Munnink[1], Marjolijn N. Lub-de Hooge[2,4], Harry Hollema[5], Johan R. de Jong[2], Igle J. de Jong[6], Sanne de Haas[7], Stefan J. Scherer[8], Wim J. Sluiter[5], Rudi A. Dierckx[2], Alfons H.H. Bongaerts[9], Jourik A. Gietema[1], and Elisabeth G.E. de Vries[1]

[1]Department of Medical Oncology, University of Groningen, University Medical Center Groningen, Groningen, The Netherlands; [2]Department of Nuclear Medicine and Molecular Imaging, University of Groningen, University Medical Center Groningen, Groningen, The Netherlands; [3]Department of Gastroenterology and Hepatology, University of Groningen, University Medical Center Groningen, Groningen, The Netherlands; [4]Department of Hospital and Clinical Pharmacy, University of Groningen, University Medical Center Groningen, Groningen, The Netherlands; [5]Department of Pathology, University of Groningen, University Medical Center Groningen, Groningen, The Netherlands; [6]Department of Urology, University of Groningen, University Medical Center Groningen, Groningen, The Netherlands; [7]F. Hoffmann-La Roche, Basel, Switzerland; [8]Genentech, San Francisco, California; and [9]Department of Radiology, University of Groningen, University Medical Center Groningen, Groningen, The Netherlands

No validated predictive biomarkers for antiangiogenic treatment of metastatic renal cell carcinoma (mRCC) exist. Tumor vascular endothelial growth factor A (VEGF-A) level may be useful. We determined tumor uptake of ^{89}Zr-bevacizumab, a VEGF-A–binding PET tracer, in mRCC patients before and during antiangiogenic treatment in a pilot study. **Methods:** Patients underwent ^{89}Zr-bevacizumab PET scans at baseline and 2 and 6 wk after initiating either bevacizumab (10 mg/kg every 2 wk) with interferon-α (3–9 million IU 3 times/wk) ($n = 11$) or sunitinib (50 mg daily, 4 of every 6 wk) ($n = 11$). Standardized uptake values were compared with plasma VEGF-A and time to disease progression. **Results:** ^{89}Zr-bevacizumab PET scans visualized 125 evaluable tumor lesions in 22 patients, with a median SUV_{max} (maximum standardized uptake value) of 6.9 (range, 2.3–46.9). Bevacizumab/interferon-α induced a mean change in tumor SUV_{max} of −47.0% (range, −84.7 to +20.0%; $P < 0.0001$) at 2 wk and an additional −9.7% (range, −44.8 to +38.9%; $P = 0.015$) at 6 wk. In the sunitinib group, the mean change in tumor SUV_{max} was −14.3% at 2 wk (range, −80.4 to +269.9; $P = 0.006$), but at 6 wk the mean change in tumor SUV_{max} was +72.6% (range, −46.4 to +236%; $P < 0.0001$) above baseline. SUV_{max} was not related to plasma VEGF-A at all scan moments. A baseline mean tumor SUV_{max} greater than 10.0 in the 3 most intense lesions corresponded with longer time to disease progression (89.7 vs. 23.0 wk; hazard ratio, 0.22; 95% confidence interval, 0.05–1.00). **Conclusion:** Tumor uptake of ^{89}Zr-bevacizumab is high in mRCC, with remarkable interpatient and intrapatient heterogeneity. Bevacizumab/interferon-α strongly decreases tumor uptake whereas sunitinib results in a modest reduction with an overshoot after 2 drug-free weeks. High baseline tumor SUV_{max} was associated with longer time to progression.

Key Words: renal cell carcinoma; molecular imaging; positron emission tomography; bevacizumab; sunitinib

J Nucl Med 2015; 56:63–69
DOI: 10.2967/jnumed.114.144840

Angiogenesis inhibitors have single-agent activity and double median progression-free survival in patients with metastatic renal cell carcinoma (mRCC) (*1–3*). However, not all patients respond, and angiogenesis inhibitors are expensive and can have side effects. Furthermore, studies indicated potential tumor-promoting effects of tyrosine kinase inhibitors (*4,5*). Therefore, it is crucial to develop a predictive biomarker for selecting patients who will benefit from these treatments. Circulating vascular endothelial growth factor A (VEGF-A) levels do not predict benefit from antiangiogenic treatment (*6–10*). VEGF-A, however, comprises different splice variants; small isoforms can diffuse freely whereas larger isoforms are primarily matrix-bound and have biologic activity in the tumor microenvironment (*11*). Local VEGF-A concentration potentially reflects whether angiogenesis drives tumor progression and might predict sensitivity to antiangiogenic treatment. Therefore, we developed the PET tracer ^{89}Zr-bevacizumab, which enables noninvasive whole-body VEGF-A imaging and quantification (*12–14*). Sunitinib and bevacizumab plus interferon-α (IFNα) are standard treatments for mRCC (*1,2*). Bevacizumab, a monoclonal antibody with a half-life of ±20 d, binds VEGF-A, thus preventing the growth factor to activate its receptor. Sunitinib is a small molecule with a half-life of ±2 d that blocks VEGF receptors and other tyrosine kinases intracellularly.

We conducted a pilot study in mRCC patients. Renal cell carcinoma (RCC) is characterized by Von Hippel–Lindau gene inactivation, resulting in high VEGF-A production and characteristic vascular tumors. The primary aim was to quantify ^{89}Zr-bevacizumab uptake in tumor lesions before treatment and changes in uptake during the early course of antiangiogenic therapy in mRCC patients. Furthermore, we wanted to explore whether ^{89}Zr-bevacizumab PET

Received Jun. 30, 2014; revision accepted Nov. 6, 2014.
For correspondence or reprints contact: Sjoukje F. Oosting, Department of Medical Oncology, University Medical Center Groningen, P.O. Box 30 001, 9700 RB Groningen, The Netherlands.
E-mail: s.oosting@umcg.nl
Published online Dec. 4, 2014.

can early identify primary resistant disease (defined as progressive disease at first evaluation), whether tumor ^{89}Zr-bevacizumab uptake correlates with plasma VEGF-A, and the effect of 2 drug-free weeks after 4 wk of sunitinib on tumor ^{89}Zr-bevacizumab uptake.

MATERIALS AND METHODS

Patients

Adult mRCC patients with measurable disease were eligible. Exclusion criteria included uncontrolled hypertension, known untreated brain metastases, clinically significant cardiovascular disease, surgery, and tyrosine kinase inhibitor treatment up to 4 wk or bevacizumab up to 4 mo before trial entry. The study was approved by the institutional review board, and all subjects signed a written informed consent form. The trial is registered with ClinicalTrials.gov (NCT00831857).

Study Design and Treatment

The primary endpoint was change of tumor standardized uptake values (SUVs) at 2 and 6 wk after the start of treatment. Patients were randomized to bevacizumab (10 mg/kg intravenously every 14 d) with IFNα (3 million IU 3 times/wk), which was increased after 2 wk to 6 and then to 9 million IU when tolerated, or sunitinib (50 mg daily orally during 4 of every 6 wk). Treatment was continued until disease progression or unacceptable toxicity. After inclusion of 3 patients, the study was amended to a nonrandomized design because of slow accrual. Because no formal comparison of treatment groups was planned, randomization was not essential for conduct of the study. The secondary endpoint was progressive disease at 3 mo according to the Response Evaluation Criteria in Solid Tumors, version 1.1 (RECIST1.1).

Imaging Techniques

Patients underwent ^{89}Zr-bevacizumab PET imaging at baseline and 2 and 6 wk after the start of treatment. PET scanning was performed 4 d after intravenous administration of 37 MBq of ^{89}Zr-bevacizumab (5 mg protein dose). Two weeks was the minimum interval required to avoid interference of activity of the first ^{89}Zr-bevacizumab injection. Six weeks was chosen to explore a rebound phenomenon after 2 sunitinib-free weeks and to explore whether a scan after 3 therapeutic bevacizumab doses shows a further change. Conjugation and labeling were done as described earlier (*13*). Patients were scanned from the upper thigh to the head in up to 8 consecutive bed positions, with a final reconstruction resolution of approximately 11 mm. Patients underwent routine CT imaging at baseline and every 3 mo thereafter. CT was performed with intravenous contrast with a maximal slice thickness of 5.0 mm (supplemental methods [available at http://jnm.snmjournals.org]). In the case of symptoms, bone scintigraphy and MR imaging were performed.

Imaging Data Analysis

Baseline PET scans were qualitatively assessed by a nuclear medicine physician and fused with the baseline CT scans to verify location and anatomic substrate of hot spots. All regions with high focal tracer uptake relative to normal-organ background were considered as lesions. Lesions were defined evaluable when identified as tumor lesion on routine imaging, greater than 10 voxels, delineable from normal-organ background, and not irradiated. Quantification was performed with AMIDE Medical Image Data Examiner software (version 0.9.1; Stanford University) (*15*). Maximum and mean SUV (SUV_{max} and SUV_{mean}, respectively) were calculated for evaluable lesions and normal organs. All lesions on the baseline CT were measured for comparison with PET. Treatment response was assessed according to RECIST1.1 by a radiologist who was masked to patient characteristics and PET results.

Biomarker Analysis

Plasma VEGF-A was measured in samples drawn at days −3, 11, and 39 before tracer administration and stored at −80°C until analysis. Samples were analyzed with the immunologic multiparametric chip technique (*7*).

Statistical Assessments

We assumed that the difference in SUV between the baseline scan and the scan after 2 and 6 wk was 1.25 SDs or greater and that there was no correlation between the first and second scans and estimated that 11 patients were required in each treatment group to predict with 80% power (2-sided $\alpha = 0.05$) that there is a true difference. To compensate for an anticipated 15% early discontinuation, 26 patients were included. For comparison of paired and nonpaired data, Wilcoxon paired-rank and the Mann–Whitney tests were used. The association between SUV_{mean} and SUV_{max} was analyzed with Spearman rank correlation and between imaging results and time to disease progression (TTP) with the Kaplan–Meier method. Analyses were performed with SPSS (version 20; IBM).

RESULTS

Patients

Between February 2009 and July 2011, 26 patients were included. Two patients did not meet eligibility criteria because of recent bevacizumab treatment and were excluded from the analysis. One patient was not evaluable, and 1 patient withdrew consent. Therefore, 22 patients, 11 per treatment group, who underwent at least the baseline and 2-wk scans, were evaluable (Supplemental Fig. 1). One patient reported nausea, redness of the face, and cold extremities for 24 h after the third tracer injection but continued bevacizumab treatment without adverse events. Patient characteristics are shown in Table 1.

Baseline ^{89}Zr-Bevacizumab PET

Normal-Organ ^{89}Zr-Bevacizumab Uptake. An example of a baseline scan is shown in Figure 1. SUV_{mean} and SUV_{max} of normal organs were strongly correlated ($r^2 = 0.99$, $P < 0.0001$, Supplemental Fig. 2A). SUV_{max} is less operator-dependent, so we used SUV_{max}. Normal-organ uptake (Fig. 2A) was consistent with a previous study (*14*) and with distribution of other antibody tracers (*16,17*).

Tumor ^{89}Zr-Bevacizumab Uptake. ^{89}Zr-bevacizumab PET visualized lesions in all patients. In total, 213 lesions were identified, of which 194 were in the field of view of the routine CT scan; 159 were also identified as tumor lesions on CT. The 35 lesions that were not detected on CT were located in the bone ($n = 12$), lymph nodes ($n = 6$), muscles ($n = 7$), kidneys ($n = 4$), and intraperitoneal ($n = 4$) and retroperitoneal compartments ($n = 2$). The 19 lesions outside the field of view of the CT scan were localized in the brain ($n = 5$ in 3 patients), bone ($n = 4$), lymph nodes ($n = 2$), and muscles ($n = 8$) (Table 2). Two patients with known brain metastases had radiotherapy before entry in the study. In the third patient, no MR imaging was performed. Sunitinib was started immediately because of rapidly progressive systemic disease without neurologic symptoms. On the CT scan, 562 lesions were identified, 145 in the bevacizumab/IFNα group and 417 in the sunitinib group, of which 231 were 10 mm or greater. The smallest lesion detected by ^{89}Zr-bevacizumab PET was 5.0 mm. The detection percentage increased with lesion size on CT (Supplemental Fig. 3); 56.7% of lesions 10 mm or greater were visible with ^{89}Zr-bevacizumab PET. The 125 tumor lesions evaluable for quantification showed a strong correlation between SUV_{mean} and SUV_{max} ($r^2 = 0.99$, $P < 0.0001$, Supplemental Fig. 2B). Therefore, only SUV_{max} is reported. Median tumor SUV_{max} was 6.9 (range, 2.3–46.9), varying from 3.8 (range, 2.7–15.4) for the patient with the lowest tumor uptake to 36.3 (range, 25.7–46.9) for the patient with the highest uptake (Fig. 2B). Furthermore, tumor tracer uptake differed according to organ localization (Fig. 2C).

TABLE 1
Patient Demographics and Clinical Characteristics

Variable	Bevacizumab/IFNα (*n* = 11)	Sunitinib (*n* = 11)	Total population (*n* = 22)
Sex			
Male	7 (64)	11 (100)	18 (82)
Female	4 (36)	0 (0)	4 (18)
Age (y)			
Median	63	57	62
Range	49–74	50–71	49–74
Nephrectomy			
Yes	7 (64)	7 (64)	14 (64)
No	4 (36)	4 (36)	8 (36)
Histology			
Pure clear cell	10 (91)	11 (100)	21 (95)
Mixed	1 (9)	0 (0)	1 (5)
Memorial Sloan Kettering Cancer Center criteria			
Good prognosis	1 (9)	1 (9)	2 (9)
Intermediate prognosis	10 (91)	10 (91)	20 (91)
World Health Organization performance			
0	10 (91)	9 (82)	19 (86)
1	1 (9)	1 (9)	2 (9)
2	0 (0)	1 (9)	1 (5)
Tumor sites			
Kidney	7 (64)	6 (55)	13 (59)
Lung	9 (82)	8 (73)	17 (77)
Lymph node	8 (73)	7 (64)	15 (68)
Bone	3 (27)	6 (55)	9 (41)
Liver	3 (27)	2 (18)	5 (23)
Pancreas	2 (18)	3 (27)	5 (23)
Adrenal	2 (18)	2 (18)	4 (18)
Other	5 (45)	5 (45)	10 (45)
No. of tumor sites			
Median	3	2	3
Range	1–4	2–6	1–6
Previous treatment			
Tyrosine kinase inhibitor	2 (18)	1 (9)	3 (14)
IFNα	0 (0)	1 (9)	1 (5)
None	9 (82)	8 (73)	16 (73)

Data are *n,* with percentages in parentheses.

Serial ^{89}Zr-Bevacizumab PET Before and During Bevacizumab/IFNα

At baseline, median SUV_{max} in 34 tumor lesions in the bevacizumab/IFNα-treated patients was 8.1 (range, 2.3–46.9). At 2 wk, a mean change of −47.0% in tumor SUV_{max} (range, −84.7 to +20.0%; $P < 0.0001$) was found, resulting in a median SUV_{max} of 4.7 (range, 1.4–10.1; Fig. 3A). This pattern was found in all patients (Supplemental Fig. 4A). Tumor SUV_{max} consistently decreased to 10 or less, even in lesions with high baseline uptake (Fig. 3B). A third ^{89}Zr-bevacizumab PET scan, available in 9 patients, showed a further mean change of −9.7% (range, −44.8 to +38.9%; $P = 0.015$) in tracer uptake in the 23 tumor lesions (Fig. 3A). Figure 4A shows an example of serial scans. Small changes over time in normal-organ ^{89}Zr-bevacizumab uptake were detected (Supplemental Fig. 5A).

Serial ^{89}Zr-Bevacizumab PET Before and During Sunitinib

Median SUV_{max} in 91 tumor lesions in patients receiving sunitinib was 6.7 at baseline (range, 2.4–34.2). After 2 wk of treatment, a mean change in tumor SUV_{max} of −14.3% was found (range, −80.4 to +269.9; $P = 0.006$), with a median SUV_{max} of 4.3 (range, 0.7–83.8) at 2 wk (Figs. 3C and 3D). At the patient level, patterns were divergent (Supplemental Fig. 4B). Mean change in tumor SUV_{max}

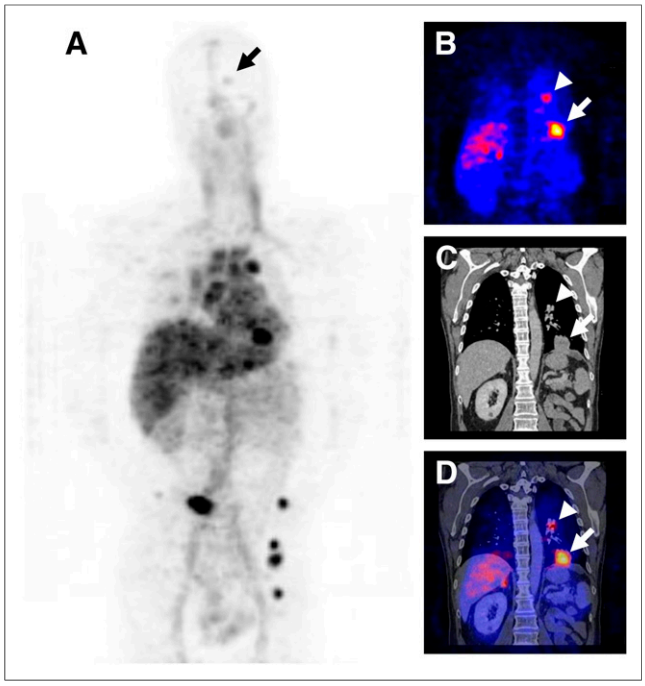

FIGURE 1. (A) Baseline ^{89}Zr-bevacizumab PET scan of mRCC patient showing tracer in blood pool and liver and metastases in bone, lung, lymph nodes, and brain (arrow). Coronal ^{89}Zr-bevacizumab PET (B), CT (C), and fusion image (D) of chest showing lung (large arrow) and lymph node (small arrow) metastases.

differed according to organ site. In kidney tumors (n = 7), a mean increase of 66.2% (range, −19.4 to +201.8%) was found, whereas in lung (n = 36) and lymph node metastases (n = 24) SUV_{max} decreased −52.3% (range, −80.4 to +8.2%; $P < 0.0001$) and −26.0% (range, −65.2 to +26.2%; P = 0.002), respectively. A third ^{89}Zr-bevacizumab PET scan in 6 patients showed 42 evaluable lesions. A mean increase of 89.3% (range, −37.2 to +411%; P = 0.0001) in tumor SUV_{max} was found after 2 sunitinib-free weeks, corresponding to a mean increase of 72.6% above baseline (range, −46.4 to +236.0%; $P < 0.0001$, Fig. 3C). Figure 4B shows an example of serial scans. Normal liver, kidney, and spleen uptake increased during sunitinib by 51.1%, 32.7%, and 25.0%, respectively, and returned to baseline after 2 drug-free weeks. In other normal organs, mean absolute changes did not exceed 1.0 SUV_{max} (Supplemental Fig. 5B).

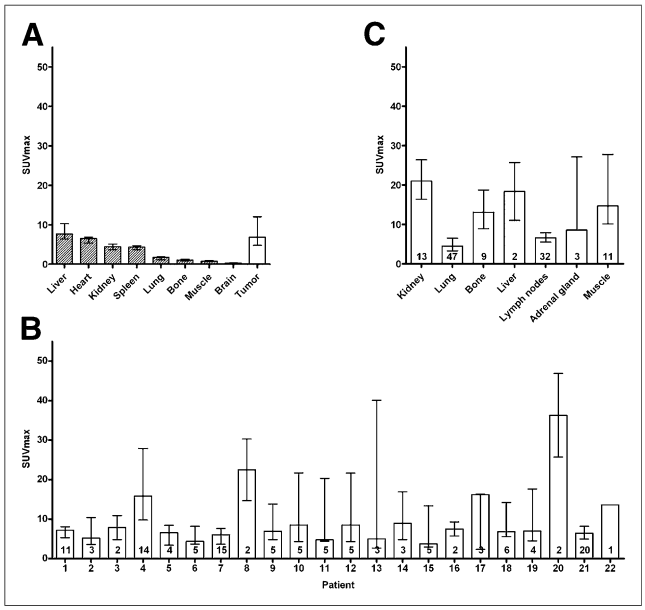

FIGURE 2. (A) Median uptake at baseline in normal organs and all evaluable tumor lesions (n = 125) on ^{89}Zr-bevacizumab PET scan, with interquartile range. Uptake in tumor lesions per patient (B) and according to organ localization (C). In bar, number of lesions is indicated.

TABLE 2
Lesions Visualized with ^{89}Zr-Bevacizumab PET and CT

Organ	PET (n)	CT (n)	Concordant (n)
Kidney	20	16 (13)*	14
Lung	54	391 (93)	54
Bone†	30	15 (11)	14
Liver	3	14 (7)	3
Lymph node†	53	86 (73)	45
Brain†	5	0 (0)	0
Adrenal gland	4	5 (5)	4
Muscle†	29	17 (15)	14
Miscellaneous	15	18 (14)	11
Total	213	562 (231)	159

*Data in parentheses for CT are for $n \geq 10$ mm.
†Including lesions outside field of view of CT scan: bone, n = 4; lymph node, n = 2; brain, n = 5; muscle, n = 8.

^{89}Zr-Bevacizumab PET and Treatment Outcome

Eighteen patients were evaluable for tumor response at 3 mo (Table 3). One patient with a sarcomatoid tumor component on bevacizumab/IFNα had progressive disease, 1 patient had a partial response, and 16 patients had stable disease. The patient with progressive disease had a mean baseline tumor SUV_{max} of 6.4, which had decreased by 34% at 2 wk. Post hoc analysis showed that 16 patients (8 of both treatment groups) with a baseline tumor SUV_{max} greater than 10.0 in the 3 most intense lesions had a longer TTP than 6 patients (3 of both treatment groups) with lower baseline tumor SUV_{max}, with a median TTP of 89.7 versus 23.0 wk (hazard ratio, 0.22; 95% confidence interval, 0.05–1.00; P = 0.050; Fig. 5). A cutoff of 10 was chosen because mean normal-organ SUV_{max} was less than 10, and bevacizumab treatment reduced tumor uptake to less than 10. Change in tumor uptake and TTP did not correlate.

Plasma VEGF-A

Baseline plasma VEGF-A (n = 20; median, 101.2 pg/mL; range, 15.4–445.1 pg/mL) did not correlate with tumor SUV_{max} and mean tumor SUV_{max} of all evaluable lesions and of the 3 most intense lesions. Plasma VEGF-A during bevacizumab treatment was unreliable and therefore not analyzed. In the sunitinib group, no relationship was found between plasma VEGF-A and tumor SUV_{max} and mean tumor SUV_{max} of all evaluable lesions and of the 3 most intense lesions at 2 and 6 wk. Also, changes in plasma VEGF-A did not correspond with changes in tumor SUV_{max} parameters.

DISCUSSION

This pilot study in 22 mRCC patients demonstrates that ^{89}Zr-bevacizumab PET visualizes tumor lesions, with major differences in tumor ^{89}Zr-bevacizumab uptake both between and within

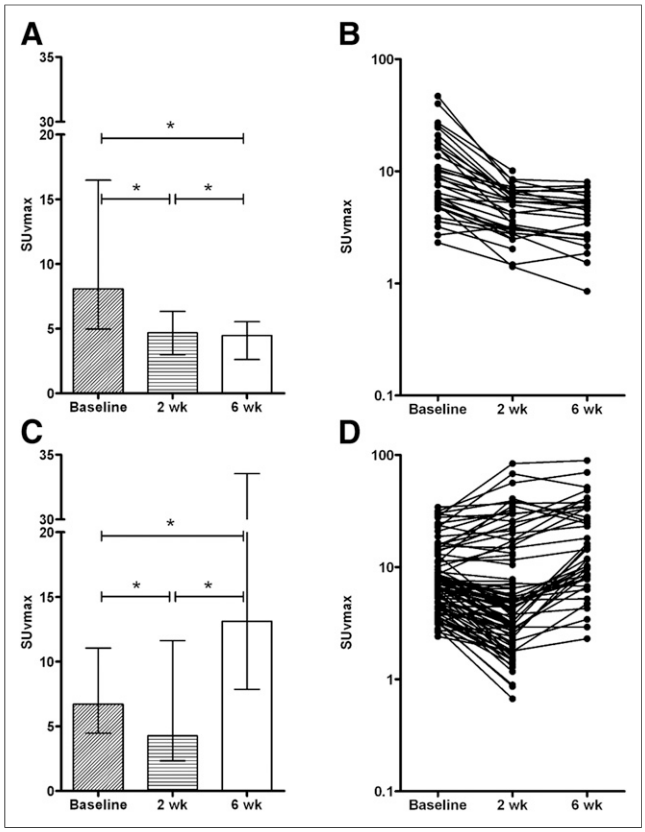

FIGURE 3. ^{89}Zr-bevacizumab tumor uptake before and during antiangiogenic treatment: 11 patients were treated with bevacizumab/IFNα (A and B) and 11 patients with sunitinib (C and D). Bars = median SUV_{max} with interquartile range; lines = individual tumor lesions. *$P < 0.05$.

patients. Antiangiogenic therapy alters tumor ^{89}Zr-bevacizumab uptake; a consistent large decrease occurs after the start of bevacizumab/IFNα and a heterogeneous response during sunitinib.

There was a striking heterogeneity in ^{89}Zr-bevacizumab tumor accumulation at baseline. In a subset of tumors, uptake did not exceed normal-organ background, reflected by visualization of only 56.7% of tumor lesions 10 mm or greater. Moreover, in evaluable lesions, large differences in SUV_{max} were found, possibly indicating a difference in biology. Tracer accumulation is dependent on delivery by tumor vasculature and on the amount of target. Heterogeneity may therefore reflect differences in vascular characteristics and tumor VEGF-A production. We did not perform biopsies in the current study. However, a correlation between ^{111}In-bevacizumab tumor uptake and VEGF-A expression in melanoma lesions and between ^{89}Zr-bevacizumab tumor uptake and VEGF-A expression in primary breast cancer has been shown previously (*13,18*).

Interpatient tumor heterogeneity is increasingly recognized and used for personalized treatment. The heterogeneity of ^{89}Zr-bevacizumab tumor uptake between patients may offer a possibility to differentiate patient groups based on tumor biology. Intrapatient tumor heterogeneity has also drawn increasing attention (*19,20*). Exome sequencing of different parts of primary RCCs and associated metastatic sites demonstrated substantial mutational heterogeneity (*19*). PET imaging has the potential to noninvasively visualize and quantify effects of mutations on expression of treatment targets across tumor lesions (*21*). Whole-body insight in heterogeneity of tumor characteristics might guide choices of drug combinations or combinations of different treatment modalities in the future.

Formal comparison of treatment groups was not the aim of this pilot study. Nevertheless, the finding of increased ^{89}Zr-bevacizumab tumor accumulation at 2 wk in a subset of lesions during sunitinib suggests a difference in biologic effect of the 2 antiangiogenic regimens, probably related to the different mechanisms of action. Unlike bevacizumab, sunitinib induces a systemic VEGF release that may be partly tumor-derived (*22,23*).

Our finding that therapeutic bevacizumab/IFNα reduced ^{89}Zr-bevacizumab tumor delivery may be explained by competition between cold and labeled antibody. However, results of preclinical and clinical studies suggest that bevacizumab-induced vascular changes are responsible (*24–26*). Two studies in mice bearing human epidermal growth factor receptor-2–expressing tumors demonstrated that VEGF-A antibody treatment reduced tumor accumulation of the human epidermal growth factor receptor-2 antibody trastuzumab and a nonspecific antibody, whereas normal-tissue distribution was not altered (*24,25*). Decreased tumor accumulation was accompanied by reduced tumor vascular density and blood flow and increased pericyte coverage of tumor vessels. Furthermore, in non–small cell lung cancer patients, tumor delivery of docetaxel diminished after 1 therapeutic bevacizumab dose, which was paralleled by reduced tumor perfusion (*26*).

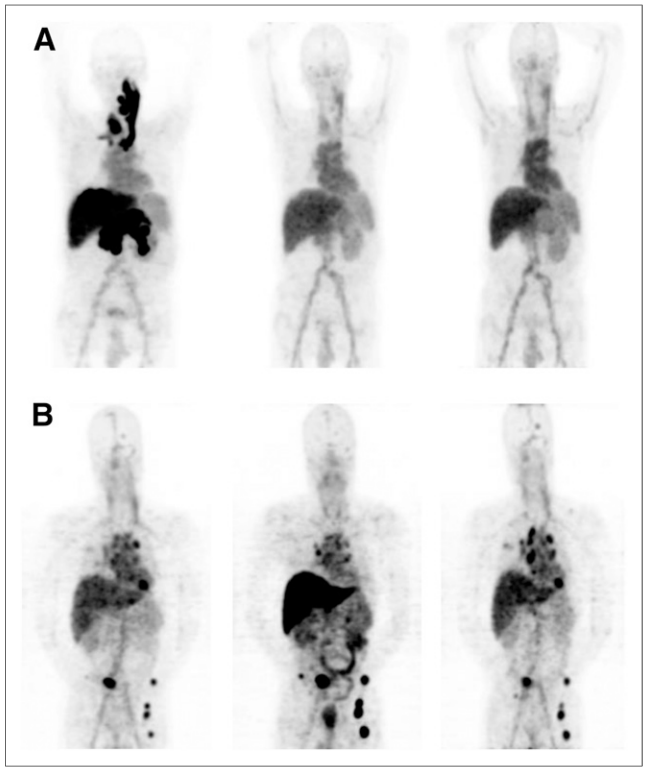

FIGURE 4. (A) Serial ^{89}Zr-bevacizumab PET scans of patient with RCC metastases in pancreas, liver, and thyroid, with associated jugular and portal vein thrombosis at baseline (left) and 2 (middle) and 6 wk (right) after start of bevacizumab/IFNα. Tumor uptake decreased whereas normal-organ uptake was stable over time. (B) Serial ^{89}Zr-bevacizumab PET scans of patient with RCC metastases in lungs, mediastinal lymph nodes, bone, and brain at baseline (left) and 2 (middle) and 6 wk (right) after start of sunitinib—that is, after 2 sunitinib-free weeks. Tumor ^{89}Zr-bevacizumab uptake decreased during treatment in lung and brain metastases but increased in normal liver and bone metastases, with reverse pattern after 2 drug-free weeks.

TABLE 3
Treatment Outcome

Variable	Bevacizumab/IFNα (n = 11)	Sunitinib (n = 11)	Total population (n = 22)
Response at 3 mo*			
Partial response	1 (9)	0 (0)	1 (5)
Stable disease	8 (73)	8 (73)	16 (73)
Progressive disease	1 (9)	0 (0)	1 (5)
Not evaluable†	1 (9)	3 (27)	4 (18)
Time to progression (wk)			
Median	23.7	30.8	23.8
Range	11.4–82.4+‡	12.9–101+‡	11.4–101+‡

*According to RECIST1.1.
†4 patients discontinued treatment because of myocardial infarction (n = 2) and hepatotoxicity (n = 1) during sunitinib and bowel perforation at metastatic site (n = 1) during bevacizumab/IFNα.
‡More than.
Data are *n,* with percentages in parentheses.

The small decrease that we observed in mean tumor ^{89}Zr-bevacizumab uptake after 2 wk of sunitinib and the rebound exceeding baseline after 2 wk off treatment correspond with our preclinical findings (*27*). Preclinical studies showed increased invasiveness and metastasis after a short sunitinib course (*4,5*). Moreover, a profound expansion of proliferating endothelial cells was demonstrated in primary RCCs after neoadjuvant sunitinib (*28*), which was not observed after bevacizumab, despite similar histologic features suggestive of vascular normalization (*28*). These findings support our observation of different tumor biology after sunitinib and bevacizumab/IFNα. Interestingly, the increased uptake in renal tumors during sunitinib treatment differs from results of ^{111}In-bevacizumab SPECT in 7 RCC patients treated with the tyrosine kinase inhibitor sorafenib for 4 wk (*29*). Reduced tumor ^{111}In-bevacizumab uptake correlated with areas of necrosis (*29*). The increase in ^{89}Zr-bevacizumab accumulation in the normal liver, spleen, and kidneys during sunitinib treatment is probably due to sunitinib-induced release of VEGF-A by normal cells. This corresponds with the observation of elevated VEGF protein in the liver, spleen, and kidney tissue of sunitinib-treated mice (*5*).

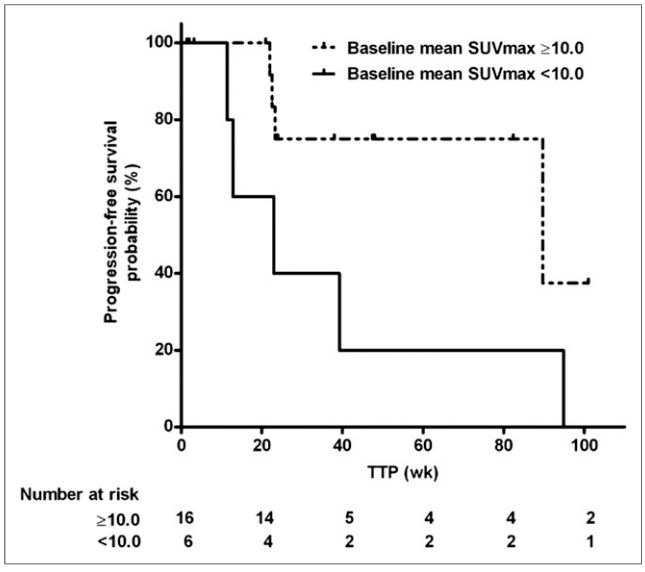

FIGURE 5. Kaplan–Meier analysis of TTP according to baseline ^{89}Zr-bevacizumab tumor uptake of 3 most intense tumor lesions. P = 0.05.

Baseline tumor ^{89}Zr-bevacizumab uptake in our study was higher than in patients with early breast cancer and in patients with metastatic neuroendocrine tumors (*13,14*). This observation probably reflects the unique pathobiology of Von Hippel–Lindau gene inactivation in RCC, resulting in high VEGF-A production by tumor cells.

We had only 1 patient with progressive disease at 3 mo, and therefore no conclusions can be drawn about the ability of ^{89}Zr-bevacizumab PET to identify primary resistant patients. Patients with intense ^{89}Zr-bevacizumab tumor accumulation at baseline had a longer TTP. This exploratory analysis should be interpreted with caution but may indicate that those tumors are more VEGF-driven and -dependent and therefore can be effectively controlled with antiangiogenic treatment.

The absence of a correlation between SUV_{max} parameters and plasma VEGF-A might be due to a different composition of circulating and microenvironmental VEGF-A isoforms.

CONCLUSION

We demonstrated heterogeneous ^{89}Zr-bevacizumab tumor uptake in mRCC patients. Bevacizumab/IFNα strongly decreases ^{89}Zr-bevacizumab tumor uptake whereas sunitinib results in modest reduction with an overshoot after 2 drug-free weeks. High baseline tumor SUV_{max} appears to be associated with longer TTP. Further studies are required to determine whether baseline ^{89}Zr-bevacizumab tumor uptake can be used to predict benefit from antiangiogenic treatment. To differentiate between prognostic and predictive value, a randomized study is required.

DISCLOSURE

The costs of publication of this article were defrayed in part by the payment of page charges. Therefore, and solely to indicate this fact, this article is hereby marked “advertisement” in accordance with 18 USC section 1734. This research was supported by a grant from F. Hoffmann-La Roche to the University Medical Center

Groningen. Sanne de Haas is an employee of Roche. Stefan J. Scherer is a former employee of Genentech. Jourik A. Gietema and Elisabeth G.E. de Vries had research grants from Roche, which were made available to the UMCG. Elisabeth G.E. de Vries served as an advisory board member of Roche-Genentech. No other potential conflict of interest relevant to this article was reported.

REFERENCES

1. Motzer RJ, Hutson TE, Tomczak P, et al. Sunitinib versus interferon alfa in metastatic renal-cell carcinoma. *N Engl J Med.* 2007;356:115–124.
2. Escudier B, Pluzanska A, Koralewski P, et al. Bevacizumab plus interferon alfa-2a for treatment of metastatic renal cell carcinoma: a randomised, double-blind phase III trial. *Lancet.* 2007;370:2103–2111.
3. Sternberg CN, Davis ID, Mardiak J, et al. Pazopanib in locally advanced or metastatic renal cell carcinoma: results of a randomized phase III trial. *J Clin Oncol.* 2010;28:1061–1068.
4. Pàez-Ribes M, Allen E, Hudock J, et al. Antiangiogenic therapy elicits malignant progression of tumors to increased local invasion and distant metastasis. *Cancer Cell.* 2009;15:220–231.
5. Ebos JM, Lee CR, Cruz-Munoz W, Bjarnason GA, Christensen JG, Kerbel RS. Accelerated metastasis after short-term treatment with a potent inhibitor of tumor angiogenesis. *Cancer Cell.* 2009;15:232–239.
6. Hegde PS, Jubb AM, Chen D, et al. Predictive impact of circulating vascular endothelial growth factor in 4 phase III trials evaluating bevacizumab. *Clin Cancer Res.* 2013;19:929–937.
7. Miles DW, de Haas SL, Dirix LY, et al. Biomarker results from the AVADO phase 3 trial of first-line bevacizumab plus docetaxel for Her2-negative metastatic breast cancer. *Br J Cancer.* 2013;108:1052–1060.
8. Escudier B, Eisen T, Stadler WM, et al. Sorafenib for treatment of renal cell carcinoma: final efficacy and safety results of the phase III treatment approaches in renal cancer global evaluation trial. *J Clin Oncol.* 2009;27:3312–3318.
9. Harmon CS, DePrimo SE, Figlin RA, et al. Circulating proteins as potential biomarkers of sunitinib and interferon-α efficacy in treatment-naïve patients with metastatic renal cell carcinoma. *Cancer Chemother Pharmacol.* 2014;73:151–161.
10. Bais C, Rabe C, Wild N, et al. Comprehensive reassessment of plasma VEGFA (pVEGFA) as a candidate predictive biomarker for bevacizumab (Bv) in 13 pivotal trials (seven indications) [abstract]. *J Clin Oncol.* 2014;32:5S.
11. Park JE, Keller GA, Ferrara N. The vascular endothelial growth factor (VEGF) isoforms: differential deposition into the subepithelial extracellular matrix and bioactivity of extracellular matrix-bound VEGF. *Mol Biol Cell.* 1993;4:1317–1326.
12. Nagengast WB, de Vries EG, Hospers GA, et al. In vivo VEGF imaging with radiolabeled bevacizumab in an ovarian tumor xenograft. *J Nucl Med.* 2007;48:1313–1319.
13. Gaykema SBM, Brouwers AH, Lub-de Hooge MN, et al. ^{89}Zr-bevacizumab PET imaging in primary breast cancer. *J Nucl Med.* 2013;54:1014–1018.
14. van Asselt SJ, Oosting SF, Brouwers AH, et al. Everolimus reduces ^{89}Zr-bevacizumab tumor uptake in patients with neuroendocrine tumors. *J Nucl Med.* 2014;55:1087–1092.
15. Loening AM, Gambhir SS. AMIDE: a free software tool for multimodality medical image analysis. *Mol Imaging.* 2003;2:131–137.
16. Dijkers EC, Oude Munnink TH, Kosterink JG, et al. Biodistribution of ^{89}Zr-trastuzumab and PET imaging of HER2-positive lesions in patients with metastatic breast cancer. *Clin Pharmacol Ther.* 2010;87:586–592.
17. Pandit-Taskar N, O'Donoghue JA, Morris MJ, et al. Antibody mass escalation study in patients with castration-resistant prostate cancer using ^{111}In-J591: lesion detectability and dosimetric projections for ^{90}Y radioimmunotherapy. *J Nucl Med.* 2008;49:1066–1074.
18. Nagengast WB, Lub-de Hooge MN, Van Straten EM, et al. VEGF-SPECT with ^{111}In-bevacizumab in stage III/IV melanoma patients. *Eur J Cancer.* 2011;47:1595–1602.
19. Gerlinger M, Rowan AJ, Horswell S, et al. Intratumor heterogeneity and branched evolution revealed by multiregion sequencing. *N Engl J Med.* 2012;366:883–892.
20. Horswell S, Matthews N, Swanton C. Cancer heterogeneity and "The struggle for existence": diagnostic and analytical challenges. *Cancer Lett.* 2013;340:220–226.
21. Petrulli JR, Sullivan JM, Zheng MQ, et al. Quantitative analysis of [^{11}C]-erlotinib PET demonstrates specific binding for activating mutations of the EGFR kinase domain. *Neoplasia.* 2013;15:1347–1353.
22. DePrimo SE, Bello CL, Smeraglia J, et al. Circulating protein biomarkers of pharmacodynamic activity of sunitinib in patients with metastatic renal cell carcinoma: modulation of VEGF and VEGF-related proteins. *J Transl Med.* 2007;5:32–42.
23. Ebos JM, Lee CR, Christensen JG, Mutsaers AJ, Kerbel RS. Multiple circulating proangiogenic factors induced by sunitinib malate are tumor-independent and correlate with antitumor efficacy. *Proc Natl Acad Sci USA.* 2007;104:17069–17074.
24. Pastuskovas CV, Mundo EE, Williams SP, et al. Effects of anti-VEGF on pharmacokinetics, biodistribution, and tumor penetration of trastuzumab in a preclinical breast cancer model. *Mol Cancer Ther.* 2012;11:752–762.
25. Arjaans M, Oude Munnink TH, Oosting SF, et al. Bevacizumab-induced normalization of blood vessels in tumors hampers antibody uptake. *Cancer Res.* 2013;73:3347–3355.
26. Van der Veldt AA, Lubberink M, Bahce I, et al. Rapid decrease in delivery of chemotherapy to tumors after anti-VEGF therapy: implications for scheduling of anti-angiogenic drugs. *Cancer Cell.* 2012;21:82–91.
27. Nagengast WB, Lub-de Hooge MN, Oosting SF, et al. VEGF-PET imaging is a non-invasive biomarker showing differential changes in the tumor during sunitinib treatment. *Cancer Res.* 2011;71:143–153.
28. Griffioen AW, Mans LA, de Graaf AM, et al. Rapid angiogenesis onset after discontinuation of sunitinib treatment of renal cell carcinoma patients. *Clin Cancer Res.* 2012;18:3961–3971.
29. Desar IME, Stillebroer AB, Oosterwijk E, et al. ^{111}In-bevacizumab imaging of renal cancer and evaluation of neoadjuvant treatment with the vascular endothelial growth factor receptor inhibitor sorafenib. *J Nucl Med.* 2010;51:1707–1715.

The Journal of NUCLEAR MEDICINE

^{89}Zr-Bevacizumab PET Visualizes Heterogeneous Tracer Accumulation in Tumor Lesions of Renal Cell Carcinoma Patients and Differential Effects of Antiangiogenic Treatment

Sjoukje F. Oosting, Adrienne H. Brouwers, Suzanne C. van Es, Wouter B. Nagengast, Thijs H. Oude Munnink, Marjolijn N. Lub-de Hooge, Harry Hollema, Johan R. de Jong, Igle J. de Jong, Sanne de Haas, Stefan J. Scherer, Wim J. Sluiter, Rudi A. Dierckx, Alfons H.H. Bongaerts, Jourik A. Gietema and Elisabeth G.E. de Vries

J Nucl Med. 2015;56:63-69.
Published online: December 4, 2014.
Doi: 10.2967/jnumed.114.144840

The Journal of Nuclear Medicine is published monthly.
SNMMI | Society of Nuclear Medicine and Molecular Imaging
1850 Samuel Morse Drive, Reston, VA 20190.
(Print ISSN: 0161-5505, Online ISSN: 2159-662X)

SNMMI SOCIETY OF NUCLEAR MEDICINE AND MOLECULAR IMAGING